The density and porosity of lunar rocks

Walter S. Kiefer

Robert J. Macke
University of Central Florida

Daniel T. Britt
University of Central Florida

Anthony J. Irving

Guy J. Consolmagno

The density and porosity of lunar rocks

Walter S. Kiefer,[1] Robert J. Macke,[2,3] Daniel T. Britt,[2] Anthony J. Irving,[4] and Guy J. Consolmagno[5]

Received 13 February 2012; accepted 7 March 2012; published 13 April 2012.

[1] Accurate lunar rock densities are necessary for constructing gravity models of the Moon's crust and lithosphere. Most Apollo-era density measurements have errors of 2–5% or more and few include porosity measurements. We report new density and porosity measurements using the bead method and helium pycnometry for 6 Apollo samples and 7 lunar meteorites, with typical grain density uncertainties of 10–30 kg m^{-3} (0.3–0.9%) and porosity uncertainties of 1–3%. Comparison between igneous grain densities and normative mineral densities show that these uncertainties are realistic and that the helium fully penetrates the pore space. Basalt grain densities are a strong function of composition, varying over at least 3270 kg m^{-3} (high aluminum basalt) to 3460 kg m^{-3} (high titanium basalt). Feldspathic highland crust has a bulk density of 2200–2600 kg m^{-3} and porosity of 10–20%. Impact basin ejecta has a bulk density of 2350–2600 kg m^{-3} and porosity of ∼20%. **Citation:** Kiefer, W. S., R. J. Macke, D. T. Britt, A. J. Irving, and G. J. Consolmagno (2012), The density and porosity of lunar rocks, *Geophys. Res. Lett.*, *39*, L07201, doi:10.1029/2012GL051319.

1. Introduction

[2] Lunar gravity observations provide our primary tool for understanding lateral variability in the structure of the Moon's crust and mantle. Accurate gravity models require the use of densities and porosities for geologically appropriate compositions. Although many bulk density measurements were reported in the Apollo-era literature, they commonly had errors of 10% or more or had no reported uncertainty [*Talwani et al.*, 1973] and are not useful for geophysical modeling. The best measurements of density use hydrostatic weighing, and the densities and porosities of 12 Apollo samples were determined by immersion in toluene [*Fujii and Osako*, 1973; *Horai and Winkler*, 1975; 1976, 1980; *Ahrens et al.*, 1977; *Jeanloz and Ahrens*, 1978; *Ahrens and Watt*, 1980]. We show below that many of those measurements have errors of 2–5% or more. Thus, there remains an important need for accurate measurements of density and porosity of lunar rocks. In this study, we report new measurements of density and porosity for 6 Apollo samples and 7 lunar meteorites, including all 3 major lunar rock types (7 mare basalts, 4 feldspathic highland rocks, 2 breccias from impact basin ejecta). The inclusion of lunar meteorites makes the results more globally representative than for Apollo samples alone [*Korotev*, 2005]. Our results include rock compositions such as high aluminum basalt, olivine gabbro, and anorthositic norite that have not previously had density and porosity measurements. These results have small uncertainties, typically 10–30 kg m^{-3}, and provide an important resource for analysis of the lunar gravity field, such as forthcoming data from the GRAIL mission.

2. Methods

[3] We measure both the bulk density, ρ_{bulk}, and the grain density, ρ_{grain}. The bulk density is the density based on the entire volume of the sample, including any pore space. The grain density is the density based solely on the solid material, excluding the pore space. Bulk density is important for calculation of gravity anomalies, and grain density is used for studying systematic trends in density as a function of rock composition. We can also calculate the porosity, $P = 1 - (\rho_{bulk}/\rho_{grain})$. The bulk volume is measured by immersion in 750-micron diameter glass beads, which provides a non-contaminating approximation of an Archimedean fluid. Grain density is measured by helium pycnometry. Full experimental details are provided by *Consolmagno et al.* [2008] and *Macke et al.* [2010]. These procedures have been applied to hundreds of meteorite samples [e.g., *Macke et al.*, 2011]. One sigma uncertainties are determined by repeated measurements of each sample. The samples reported in Table 1 ranged from 9.1 to 311 gm, with the smallest samples, 70215 and MIL 05035, having the largest measurement uncertainties. Table S1 in the auxiliary material illustrates the effect of sample size on measurement uncertainty.[1]

[4] Normative mineralogies such as the CIPW norm use simple chemical rules to combine oxide compositions into end-member mineral compositions that approximate the actual compositions of igneous rocks [e.g., *Best*, 2003]. Such normative mineral calculations can be used on igneous rocks, whose mineralogy can be assumed to be in equilibrium with its chemical composition, but should not be applied to rocks such as impact basin ejecta, whose formation involves non-equilibrium physical mixtures of unrelated rock types. Figure 1 compares the measured grain densities (porosity free) of igneous rocks from this study and from literature sources with the expected grain density based on normative mineralogy. The normative mineralogies were calculated using K. Hollacher's (Calculation of a CIPW norm from a bulk chemical analysis, 2011, available at http://minerva.union.edu/hollochk/c_petrology/norms.htm)

[1]Lunar and Planetary Institute, Houston, Texas, USA.
[2]Department of Physics, University of Central Florida, Orlando, Florida, USA.
[3]Now at Department of Physics, Boston College, Chestnut Hill, Massachusetts, USA.
[4]Department of Earth and Space Sciences, University of Washington, Seattle, Washington, USA.
[5]Vatican Observatory, Vatican City, Holy See.

0094-8276/12/2012GL051319

[1]Auxiliary materials are available in the HTML. doi:10.1029/2012GL051319.

Table 1. Density and Porosity Results[a]

Sample	Mass (gm)	Rock Type	Bulk Density	Grain Density	Porosity
12051,19	12.2	Low Ti Basalt	3270 ± 50	3320 ± 20	1.8 ± 1.7%
15555,62	33.0	Low Ti Basalt	3110 ± 30	3350 ± 10	7.1 ± 0.9%
70215,312	9.1	High Ti Basalt	3170 ± 80	3460 ± 50	8.3 ± 2.7%
LAP 02205,72	25.0	Low Ti Basalt	3010 ± 40	3350 ± 20	10.3 ± 1.4%
MIL 05035,51	9.3	Low Ti Basalt	3240 ± 100	3350 ± 50	3.4 ± 3.2%
NWA 2977	19.1	Olivine Gabbro	3130 ± 60	3410 ± 20	8.3 ± 1.9%
NWA 4898	19.1	Hi Al Basalt	3030 ± 40	3270 ± 10	7.2 ± 1.2%
12063,74[b]		*Low Ti Basalt*	*3210 ± 30*	*3360 ± 10*	*4.7 ± 1.0%*
15418,179	26.7	Anorthositic Norite	2810 ± 20	2900 ± 10	3.2 ± 0.9%
NWA 482	311.5	Anorthositic Norite	2510 ± 20	2840 ± 10	11.5 ± 0.8%
NWA 4932	24.5	Noritic Anorthosite	2840 ± 40	2910 ± 10	2.2 ± 1.5%
NWA 5000	16.4	Anorthositic Norite	2610 ± 30	2870 ± 30	9.2 ± 1.4%
60025,36[c]		*Ferroan Anorthosite*	*2200–2240*	*>2710–2750*	*>18–20%*
14303,14	22.3	Fra Mauro Formation	2520 ± 30	3050 ± 10	17.5 ± 1.0%
14321,220	10.0	Fra Mauro Formation	2360 ± 40	3030 ± 30	22.1 ± 1.5%
72395,14[d]	*3.7*	*Impact Melt Breccia*	*2540*	*>3070*	*>17.4%*
77035,44[d]	*3.7*	*Impact Melt Breccia*	*2620*	*>3050*	*>14.1%*

[a]Samples starting with numbers are Apollo samples, samples starting with letters are meteorites. Densities are reported in kg m^{-3}. Italicized rows indicate toluene immersion results from the literature and should typically be interpreted as lower bounds on the true grain density and porosity of each sample. All other rows are helium pycnometry and bead method results from this study.
[b]From *Ahrens and Watt* [1980].
[c]From *Jeanloz and Ahrens* [1978].
[d]From *Horai and Winkler* [1976].

implementation of the CIPW norm, using chemical compositions from Table S2. In all cases, the helium pycnometry results plot very close to the theoretically expected density. This shows that our error bars, although quite small, are nevertheless realistic estimates of the uncertainty in the measurements. This also means that the helium fully penetrates the pore space in these samples, with no unmeasured sealed pores (if such unmeasured porosity existed, our grain densities would be less than the normative densities). The complete penetration of the pore space reflects the existence of a network of impact-induced micro-fractures in the lunar rocks, which can be penetrated by helium's small atomic radius. Based on the significant figures reported for density and porosity measurements in toluene, the presumed precision of those measurements was 1 kg m^{-3} for grain density and 0.1% for porosity [e.g., *Fujii and Osako*, 1973; *Horai and Winkler*, 1975]. However, Figure 1 shows that the actual errors in ρ_{grain} by toluene immersion are usually 80–170 kg m^{-3} (2–5%), corresponding to similar percentage errors in porosity. This is due to the inability of the toluene in most cases to fully penetrate the pore space in these samples. In two cases out of nine, 12063 and 70215 [*Ahrens and Watt*, 1980; *Horai and Winkler*, 1976], the toluene measurements do agree well with the normative densities.

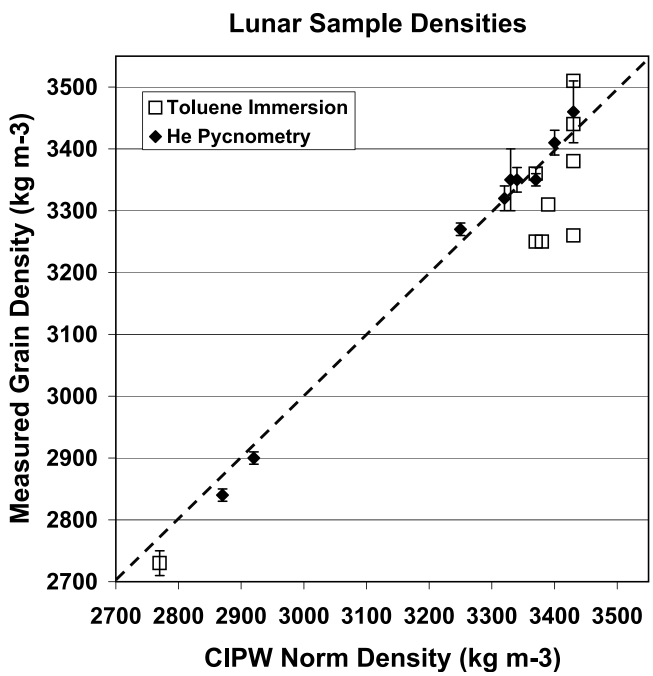

Figure 1. Measured grain density versus the normative mineralogy density for basalts and gabbros measured by helium pycnometry (filled diamonds) and by toluene immersion (open squares). Normative mineralogy densities are from Table S2. Grain densities by He pycnometry are from Table 1. Grain densities by toluene immersion are from *Fujii and Osako* [1973], *Horai and Winkler* [1975, 1976, 1980], *Ahrens et al.* [1977], *Jeanloz and Ahrens* [1978], and *Ahrens and Watt* [1980]. The dashed line represents perfect agreement between the measured and theoretical densities.

3. Results

3.1. Basalts

[5] The primary chemical classification applied to lunar mare basalts is low Ti versus high Ti, although even low Ti mare basalts are high in Ti by terrestrial basalt standards. Important secondary classifications include the amount of Mg, either as the MgO concentration or as Mg#, which is the molar ratio MgO/(MgO + FeO), and the abundance of Al [*Neal and Taylor*, 1992; *Papike et al.*, 1998]. All three of these geochemical factors are important to the overall grain density of basalts. Other chemical variations, such as low K versus high K, are unlikely to be important for density. We

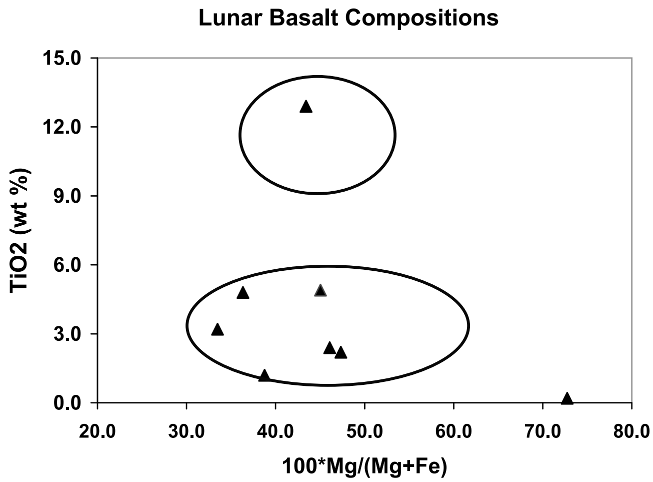

Figure 2. The chemical classification of basalts and gabbros from Table 1 in terms of Mg# and TiO_2 abundance. The ovals encompass the range of compositions measured for mare basalt samples collected during the Apollo program [*Neal and Taylor*, 1992].

have measured mare basalts with a broad range of compositions (Figure 2). Our results demonstrate a strong dependence of ρ_{grain} on chemical composition (Table 1). High Al basalt Northwest Africa (NWA) 4898 has a high abundance of Al_2O_3 and thus of the low-density mineral plagioclase [*Greshake et al.*, 2008], and has a grain density of only 3270 kg m^{-3}. The low Ti basalts in Table 1 [*Neal et al.*, 1994; *Ryder and Schuraytz*, 2001; *Zeigler et al.*, 2005; *Joy et al.*, 2008] form a tight cluster with ρ_{grain} = 3350 kg m^{-3}. High Ti basalt 70215 contains a high abundance of dense ilmenite (13%) and only 18% plagioclase [*Dymek et al.*, 1975], resulting in high ρ_{grain} of 3460 kg m^{-3} , which is consistent with the toluene-immersion result of *Horai and Winkler* [1976]. NWA 2977, an olivine gabbro interpreted as a shallow cumulate, consists mainly of olivine and pyroxene with only about 10% plagioclase [*Jolliff et al.*, 2003; *Bunch et al.*, 2006] with a relatively high density of 3410 kg m^{-3}. All of the basalt densities in Table 1 are significantly larger than for terrestrial basalts, reflecting the much higher abundance of FeO in lunar basalts than in terrestrial basalts. For a typical mare porosity of ~7% (range 2–10%, Table 1), the bulk density (which is the relevant parameter for gravity models) varies between 3010 and 3270 kg m^{-3}.

[6] Mare basalts have a relatively simple mineralogy, dominated by plagioclase, pyroxene, olivine and ilmenite. It is therefore reasonable to consider if the grain density is controlled by just a few chemical components. Fe and Mg control the density of pyroxene and olivine, Al controls the abundance of low density plagioclase, and Ti controls the abundance of high density ilmenite. We have calculated least squares regressions between basalt grain densities from Table 1 and various choices of 1 and 2 chemical components, selected from Al_2O_3, FeO, MgO, and TiO_2. The best fit involves TiO_2 and Al_2O_3 (in weight %):

$$\rho_{grain} = 3470 + 10.8\ TiO_2 - 17.7\ Al_2O_3. \quad (1)$$

This relationship has an RMS density misfit of 17 kg m^{-3}, which is comparable to the uncertainties in the measured grain densities, and it accounts for 91% of the total variance in the raw density data. The best single component fit is for Al_2O_3, which accounts for 39% of the data variance.

3.2. Highland Crust

[7] The Moon's highland crust formed from the crystallization of the lunar magma ocean. Its upper part is composed predominantly of plagioclase, averaging 80 volume per cent, with a smaller amount of mafic minerals [*Warren*, 1993; *Taylor*, 2009]. The mafic minerals have varying relative abundances of Mg and Fe; differences between Apollo samples and lunar meteorites suggest the possibility of regional variability of the Mg# in the lunar highland crust [*Korotev et al.*, 2003]. Rocks in the upper part of the highlands crust have experienced ~4 billion years of impact bombardment, and thus have suffered varying degrees of impact brecciation and shock melting.

[8] For gravity modeling, it is important to know the bulk density of the upper-most part of the highland crust for calculating the gravitational effect of the Moon's topography (the Bouguer correction). Table 1 includes measurements of several samples that are predominantly composed of calcium-rich plagioclase (anorthite), which we interpret as samples of the Moon's feldspathic highland crust. They vary in bulk composition between 22 to 35 weight percent Al_2O_3 (60–95% anorthite), with Mg# between 42 and 66; grain densities are lowest for the most plagioclase rich rocks. The nomenclature used in Table 1 is for the igneous composition based on the work by *Stöffler et al.* [1980], although each of these rocks has experienced substantial post-igneous crystallization processing, such as brecciation, shock melting, thermal annealing, and addition of meteoritic material [*Nord et al.*, 1977; *Ryder*, 1982; *Daubar et al.*, 2002; *Irving et al.*, 2008; *Korotev et al.*, 2009]. Based on this range of compositions, these samples provide an initial estimate of the likely range of densities for the uppermost part of the Moon's highland crust. The measured grain density of 60025 [*Jeanloz and Ahrens*, 1978] is only slightly higher than the normative density (Figure 1), so its porosity is probably close to the measured toluene-immersion value of 20%. The porosity of 15418, 3%, is small because of post-crystallization thermal annealing to a granulite texture [*Nord et al.*, 1977], and our measured bulk density is consistent with that of *Todd et al.* [1972]. The porosities of the 3 feldspathic meteorites, NWA 482, NWA 4932, and NWA 5000 range between 2 and 11.5%. Meteorite porosities may be reduced during ejection from the Moon or landing on Earth [*Warren*, 2001], so these values may be lower bounds on the true porosity of the highland crust. This suggests that a reasonable range for the bulk density of the uppermost highland crust is between 2200 and 2600 kg m^{-3}; porosity at the high end of the measured range favors lower values of bulk density. This estimate may be improved by on-going analysis of additional samples.

3.3. Impact Breccias

[9] The Fra Mauro Formation consists of material ejected by the impact that formed the Imbrium basin. Imbrium ejecta is widely distributed across the Moon's near side [*Wilhelms and McCauley*, 1971; *Spudis et al.*, 2011] and is a possible analog for ejecta units from other impact basins. Table 1 includes two breccias from the Fra Mauro Formation,

14303 and 14321. Based on sample petrology, they are classified as crystalline matrix breccias and interpreted as ejecta from the Imbrium basin impact [*Simonds et al.*, 1977]. 14321 was collected on the rim of Cone Crater and likely originated 70–80 meters below the local surface. 14303 was collected at a distance of 1.5 km from the crater rim and likely samples the top part of the ejecta deposit's stratigraphy [*Swann et al.*, 1977]. The two samples have identical grain densities, 3030–3050 kg m^{-3}, and similar porosities (17–22%, Table 1) and thus provide a concordant but limited sampling of the properties of the upper 80 meters of the ejecta deposit's stratigraphic column. Independent measurements of the bulk density of other pieces of 14321 by *Chung et al.* [1972] and *Mizutani and Newbigging* [1973] are 2350 and 2400 kg m^{-3} respectively, consistent with our value in Table 1.

[10] *Horai and Winkler* [1976] measured two impact melt breccias from the South and North massifs of the Serenitatis basin rim at the Apollo 17 landing site, 72395 and 77035. Their measured grain densities overlap our uncertainties for 14303 and 14321, although their results should be regarded as lower bounds because they are based on toluene immersion. For gravity modeling, the bulk density is the important parameter, and the combined range of the results summarized here is 2350–2600 kg m^{-3}, similar to the range suggested above for the highland crust. Porosities are in the range 15–22% (Table 1).

4. Summary and Implications

[11] Only 12 hydrostatic measurements of density and porosity of lunar rocks were made during the Apollo era, and many of those measurements systematically underestimate the true grain density and porosity of the samples. In this work, we report new density and porosity measurements by helium pycnometry of 13 lunar samples, covering the full range of major rock types, including several previously unmeasured types. These measurements are the most accurate existing data set of lunar density and porosity, with typical uncertainties of 10–30 kg m^{-3} for grain density and 1–3% for porosity.

[12] The results show the systematic dependence of density on composition and will benefit lunar gravity studies in a variety of ways. For example, a recent gravity model of the Marius Hills required both the density of the basalt and the porosity of the highland crust as model parameters [*Kiefer*, 2010]. Due to lack of sample data, previous studies of lunar mascons have typically used a single density for all mare basalts [e.g., *Neumann et al.*, 1996; *Hikida and Wieczorek*, 2007], but our results (equation (1)) combined with remote sensing data [*Prettyman et al.*, 2006; *Kramer et al.*, 2008; *Staid et al.*, 2011] will allow models that account for regional variations in basalt composition, providing a sharper view of subsurface structures such as mascons. Cryptomare are ancient deposits of mare basalt that were later covered by a blanket of impact basin ejecta [*Schultz and Spudis*, 1979]. Cryptomare are presently mapped geologically and spectrally in places such as Schiller-Schickard by limited exposures of the mostly buried basalt [e.g., *Blewett et al.*, 1995]. Because the bulk density of mare basalt is considerably larger than impact basin ejecta, cryptomare deposits should stand out as local gravity highs. Gravity models thus may be a useful tool in defining the spatial distribution and thickness of buried cryptomare, and will therefore help to better define the early stages of the Moon's volcanic history. Quantitative gravity models of cryptomare require knowledge of the densities of both the basalt and the basin ejecta, which our results provide.

[13] **Acknowledgments.** We thank Randy Korotev and an anonymous reviewer for reviews that improved the manuscript and the NASA CAPTEM and Meteorite Working Group, Carl Agee, Ted Bunch, Art Ehlmann, Ansgar Greshake, Gregory Hupé, and Philip Mani for access to samples. This work was supported by NASA grants NNX11AF70G, NNX09AD91G, and NASA Cooperative Agreement NNX08AC28A. Lunar and Planetary Institute contribution 1658.

References

Ahrens, T. J., and J. P. Watt (1980), Dynamic properties of mare basalts: Relation of equations of state to petrology, *Proc. Lunar Planet. Sci. Conf.*, *11th*, 2059–2074.

Ahrens, T. J., I. Jackson, and R. Jeanloz (1977), Shock compression and adiabatic release of a titaniferous mare basalt, *Proc. Lunar Sci. Conf.*, *8th*, 3437–3455.

Best, M. G. (2003), *Igneous and Metamorphic Petrology*, 2nd ed., Blackwell, Malden, Mass.

Blewett, D. T., B. R. Hawke, P. G. Lucey, G. J. Taylor, R. Jaumann, and P. D. Spudis (1995), Remote sensing and geologic studies of the Schiller-Schickard region of the Moon, *J. Geophys. Res.*, *100*, 16,959–16,977, doi:10.1029/95JE01409.

Bunch, T. E., J. H. Wittke, R. L. Korotev, and A. J. Irving (2006), Lunar meteorites NWA 2700, NWA 2727 and NWA 2977: Mare basalt/gabbro breccias with affinities to NWA 773, *Lunar Planet. Sci. Conf.*, *37th*, Abstract 1375.

Chung, D. H., W. B. Westphal, and G. R. Olhoeft (1972), Dielectric properties of Apollo 14 lunar samples, *Proc. Lunar Sci. Conf.*, *3rd*, 3161–3172.

Consolmagno, G. J., D. T. Britt, and R. J. Macke (2008), The significance of meteorite density and porosity, *Chem. Erde*, *68*, 1–29, doi:10.1016/j.chemer.2008.01.003.

Daubar, I. J., D. A. Kring, T. D. Swindle, and A. J. T. Jull (2002), Northwest Africa 482: A crystalline impact-melt breccia from the lunar highlands, *Meteorit. Planet. Sci.*, *37*, 1797–1813, doi:10.1111/j.1945-5100.2002.tb01164.x.

Dymek, R. F., A. L. Albee, and A. A. Chodos (1975), Comparative mineralogy and petrology of Apollo 17 mare basalts: Samples 70215, 71055, 74255, and 75055, *Proc. Lunar Sci. Conf.*, *6th*, 49–77.

Fujii, N., and M. Osako (1973), Thermal diffusivity of lunar rocks under atmospheric and vacuum conditions, *Earth Planet. Sci. Lett.*, *18*, 65–71, doi:10.1016/0012-821X(73)90035-6.

Greshake, A., A. J. Irving, S. M. Kuehner, R. L. Korotev, M. Gellissen, and H. Palme (2008), Northwest Africa 4898: A new high-alumina mare basalt from the Moon, *Lunar Planet. Sci. Conf.*, *39th*, Abstract 1631.

Hikida, H., and M. A. Wieczorek (2007), Crustal thickness of the Moon: New constraints from gravity inversions using polyhedral shape models, *Icarus*, *192*, 150–166, doi:10.1016/j.icarus.2007.06.015.

Horai, K., and J. L. Winkler (1975), Thermal diffusivity of lunar rock sample 12002,85, *Proc. Lunar Sci. Conf.*, *6th*, 3207–3215.

Horai, K., and J. L. Winkler (1976), Thermal diffusivity of four Apollo 17 rock samples, *Proc. Lunar Sci. Conf.*, *7th*, 3183–32,204.

Horai, K., and J. L. Winkler (1980), Thermal diffusivity of two Apollo 11 samples, 10020,44 and 10065,23: Effect of petrofabrics on the thermal conductivity of porous lunar rocks under vacuum, *Proc. Lunar Planet. Sci. Conf.*, *11th*, 1777–1788.

Irving, A. J., S. M. Kuehner, R. L. Korotev, D. Rumble, and A. C. Hupé (2008), Petrology and bulk composition of large lunar feldspathic leucogabbroic breccia northwest Africa 5000, *Lunar Planet. Sci. Conf.*, *39th*, Abstract 2168.

Jeanloz, R., and T. J. Ahrens (1978), The equation of state of a lunar anorthosite: 60025, *Proc. Lunar Planet. Sci. Conf.*, *9th*, 2789–2803.

Jolliff, B. L., R. L. Korotev, R. A. Zeigler, and C. Floss (2003), Northwest Africa 773: Lunar mare breccia with a shallow-formed olivine-cumulate component, inferred very-low-Ti heritage, and a KREEP connection, *Geochim. Cosmochim. Acta*, *67*, 4857–4879, doi:10.1016/j.gca.2003.08.012.

Joy, K. H., I. A. Crawford, M. Anand, R. C. Greenwood, I. A. Franchi, and S. S. Russell (2008), The petrology and geochemistry of Miller Range 05035: A new lunar gabbroic meteorite, *Geochim. Cosmochim. Acta*, *72*, 3822–3844, doi:10.1016/j.gca.2008.04.032.

Kiefer, W. S. (2010), Gravity constraints on the subsurface structure of the Marius Hills: A sharper view of the magmatic plumbing system based on

improved topography data and new lunar density measurements, *Lunar Planet. Sci. Conf.*, *41st*, Abstract 1274.
Korotev, R. L. (2005), Lunar geochemistry as told by lunar meteorites, *Chem. Erde*, *65*, 297–346, doi:10.1016/j.chemer.2005.07.001.
Korotev, R. L., B. L. Jolliff, R. A. Zeigler, J. J. Gillis, and L. A. Haskin (2003), Feldspathic lunar meteorites and their implications for compositional remote sensing of the lunar surface and the composition of the lunar crust, *Geochim. Cosmochim. Acta*, *67*, 4895–4923, doi:10.1016/j.gca.2003.08.001.
Korotev, R. L., R. A. Zeigler, B. L. Jolliff, A. J. Irving, and T. E. Bunch (2009), Compositional and lithological diversity among brecciated lunar meteorites of intermediate iron concentration, *Meteorit. Planet. Sci.*, *44*, 1287–1322, doi:10.1111/j.1945-5100.2009.tb01223.x.
Kramer, G. Y., B. L. Jolliff, and C. R. Neal (2008), Distinguishing high-alumina mare basalts using Clementine UVVIS and Lunar Prospector GRS data: Mare Moscoviense and Mare Nectaris, *J. Geophys. Res.*, *113*, E01002, doi:10.1029/2006JE002860.
Macke, R. J., D. T. Britt, and G. J. Consolmagno (2010), Analysis of systematic error in "bead method" measurements of meteorite bulk volume and density, *Planet. Space Sci.*, *58*, 421–426, doi:10.1016/j.pss.2009.11.006.
Macke, R. J., D. T. Britt, and G. J. Consolmagno (2011), Density, porosity, and magnetic susceptibility of achondritic meteorites, *Meteorit. Planet. Sci.*, *46*, 311–326, doi:10.1111/j.1945-5100.2010.01155.x.
Mizutani, H., and D. F. Newbigging (1973), Elastic wave velocities of Apollo 14, 15, and 16 rocks, *Proc. Lunar Sci. Conf.*, *4th*, 2601–2609.
Neal, C. R., and L. A. Taylor (1992), Petrogenesis of mare basalts: A record of lunar volcanism, *Geochim. Cosmochim. Acta*, *56*, 2177–2211, doi:10.1016/0016-7037(92)90184-K.
Neal, C. R., M. D. Hacker, G. A. Snyder, L. A. Taylor, Y.-G. Liu, and R. A. Schmitt (1994), Basalt generation at the Apollo 12 site, Part I: New data, classification, and re-evaluation, *Meteoritics*, *29*, 334–348.
Neumann, G. A., M. T. Zuber, D. E. Smith, and F. G. Lemoine (1996), The lunar crust: Global structure and signature of major basins, *J. Geophys. Res.*, *101*, 16,841–16,843, doi:10.1029/96JE01246.
Nord, G. L., J. M. Christie, J. S. Lally, and A. H. Heuer (1977), The thermal and deformational history of Apollo 15418, a partly shock-melted lunar breccia, *Moon*, *17*, 217–231, doi:10.1007/BF00562197.
Papike, J. J., G. Ryder, and C. K. Shearer (1998), Lunar samples, in *Planetary Materials*, *Rev. Mineral.*, vol. 36, pp. 1–234, Mineral. Soc. of Am., Washington, D. C.
Prettyman, T. H., J. J. Hagerty, R. C. Elphic, W. C. Feldman, D. J. Lawrence, G. W. McKinney, and D. T. Vaniman (2006), Elemental composition of the lunar surface: Analysis of gamma ray spectroscopy data from Lunar Prospector, *J. Geophys. Res.*, *111*, E12007, doi:10.1029/2005JE002656.
Ryder, G. (1982), Lunar anorthosite 60025, the petrogenesis of anorthosites, and the composition of the Moon, *Geochim. Cosmochim. Acta*, *46*, 1591–1601, doi:10.1016/0016-7037(82)90316-7.
Ryder, G., and B. C. Schuraytz (2001), Chemical variation of the large Apollo 15 olivine-normative mare basalt rock samples, *J. Geophys. Res.*, *106*, 1435–1451, doi:10.1029/2000JE001368.
Schultz, P. H., and P. D. Spudis (1979), Evidence for ancient mare volcanism, *Proc. Lunar Planet. Sci. Conf.*, *10*, 2899–2918.
Simonds, C. H., W. C. Phinney, J. L. Warner, P. E. McGee, J. Geeslin, R. W. Brown, and J. M. Rhodes (1977), Apollo 14 revisited, or breccias aren't so bad after all, *Proc. Lunar Sci. Conf.*, *8th*, 1869–1893.
Spudis, P. D., D. E. Wilhelms, and M. S. Robinson (2011), The Sculptured Hills of the Taurus Highlands: Implications for the relative age of Serentitatis, basin chronologies and the cratering history of the Moon, *J. Geophys. Res.*, *116*, E00H03, doi:10.1029/2011JE003903.
Staid, M. I., et al. (2011), The mineralogy of late stage lunar volcanism as observed by the Moon Mineralogy Mapper on Chandrayaan-1, *J. Geophys. Res.*, *116*, E00G10, doi:10.1029/2010JE003735.
Stöffler, D., H.-D. Knöll, U. B. Marvin, C. H. Simonds, and P. H. Warren (1980), Recommended classification and nomenclature of lunar highland rocks—A committee report, in *Proceedings of the Conference on Lunar Highlands Crust*, edited by J. J. Papike and R. B. Merrill, pp. 51–70, Pergamon, New York.
Swann, G. A., et al. (1977), *Geology of the Apollo 14 Landing Site in the Fra Mauro Highlands*, *U.S. Geol. Soc. Prof. Pap.*, *880*, 103 pp.
Talwani, M., G. Thompson, B. Dent, H.-G. Kahle, and S. Buck (1973), Traverse Gravimeter Experiment, in *Apollo 17 Preliminary Science Report*, *NASA Spec. Publ.*, *SP-330*, 1–13.
Taylor, G. J. (2009), Ancient lunar crust: Origin, composition, and implications, *Elements*, *5*, 17–22, doi:10.2113/gselements.5.1.17.
Todd, T., H. Wang, W. S. Baldridge, and G. Simmons (1972), Elastic properties of Apollo 14 and 15 rocks, *Proc. Lunar Sci. Conf.*, *3rd*, 2577–2586.
Warren, P. H. (1993), A concise compilation of petrologic information on possibly pristine nonmare Moon rocks, *Am. Mineral.*, *78*, 360–376.
Warren, P. H. (2001), Porosities of lunar meteorites: Strength, porosity, and petrologic screening during the meteorite delivery process, *J. Geophys. Res.*, *106*, 10,101–10,111, doi:10.1029/2000JE001283.
Wilhelms, D. E., and J. F. McCauley (1971), Geologic map of the near side of the Moon, *U.S. Geol. Surv. Misc. Invest. Map*, *I-703*.
Zeigler, R. A., R. L. Korotev, B. L. Jolliff, and L. A. Haskin (2005), Petrography and geochemistry of the LaPaz Icefield basaltic lunar meteorite and source crater pairing with northwest Africa 032, *Meteorit. Planet. Sci.*, *40*, 1073–1101, doi:10.1111/j.1945-5100.2005.tb00174.x.

D. T. Britt, Department of Physics, University of Central Florida, 4000 Central Florida Blvd., Orlando, FL 32816, USA.
G. J. Consolmagno, Vatican Observatory, V-00120 Vatican City, Holy See.
A. J. Irving, Department of Earth and Space Sciences, University of Washington, Seattle, WA 98195, USA.
W. S. Kiefer, Lunar and Planetary Institute, 3600 Bay Area Blvd., Houston, TX 77058, USA. (kiefer@lpi.usra.edu)
R. J. Macke, Department of Physics, Boston College, Chestnut Hill, MA 02467, USA.